

# An analysis of pavement heat flux to optimize the water efficiency of a pavement-watering method

Martin HENDEL<sup>1,2,3\*</sup>, Morgane COLOMBERT<sup>2</sup>, Youssef DIAB<sup>2,4</sup>, Laurent ROYON<sup>3</sup>

<sup>1</sup>Paris City Hall, Water and Sanitation Department, F-75014, Paris, France

<sup>2</sup>Université Paris-Est, EIVP, F-75019, Paris, France

<sup>3</sup>Univ Paris Diderot, Sorbonne Paris Cité, Laboratory MSC, UMR 7057, CNRS, F-75013, Paris, France

<sup>4</sup>Université Paris-Est, LEESU-GU, UMR MA 120, F-77420, Champs-sur-Marne, France

\* (corresponding author: [martin.hendel@paris.fr](mailto:martin.hendel@paris.fr))

Preprint version. Uploaded on May 12<sup>th</sup>, 2014.

**Abstract:** Pavement-watering as a technique of cooling dense urban areas and reducing the urban heat island effect has been studied since the 1990's. The method is currently considered as a potential tool for and climate change adaptation against increasing heat wave intensity and frequency. However, although water consumption necessary to implement this technique is an important aspect for decision makers, optimization of possible watering methods has only rarely been conducted. We propose an analysis of pavement heat flux at a depth of 5 cm and solar irradiance measurements to attempt to optimize the watering period, cycle frequency and water consumption rate of a pavement-watering method applied in Paris over the summer of 2013. While fine-tuning of the frequency can be conducted on the basis of pavement heat flux observations, the watering rate requires a heat transfer analysis based on a relation established between pavement heat flux and solar irradiance during pavement insolation. From this, it was found that watering conducted during pavement insolation could be optimized to a frequency of every 30 minutes and water consumption could be reduced by more than 76% while reducing the cooling effect by less than 10%.

## Keywords

Evaporative cooling; pavement heat flux; pavement-watering; urban heat island; climate change adaptation; heat wave

## 1. Introduction

Watering horizontal or vertical urban surfaces as a method for cooling urban spaces has been studied in Japan since the 1990s [1]–[7] and is only a recent topic in French cities such as Paris and Lyon [8]–[10]. With reported air temperature reductions ranging from 0.4°C at 2 m [9] to 4°C at 0.9 m [3], this technique is viewed as an efficient means of reducing urban heat island (UHI) intensity. In France and especially Paris, the predicted increases in heat wave intensity and frequency due to climate change [11], combined with the high sensitivity of dense cities to such episodes [12], have focused efforts on the development of appropriate adaptation tools. In parallel to techniques such as green space development, pavement-watering is seen as one of these potential tools for heat-wave adaptation in mineral areas.

Pavement-watering implies the choice of a watering method and a corresponding urban infrastructure. For any given target-area, every watering method can be characterized by three parameters: the watering period, the watering rate and the watering frequency. The former indicates the period of each day during which pavement-watering is active, the second is the average amount of water delivered per unit area and per unit time (expressed in  $mm/h$ , equivalent to  $l/m^2.h$ ) and the last indicates the frequency of the watering cycles. Of these parameters, the watering rate is the one that defines the method's water consumption and is

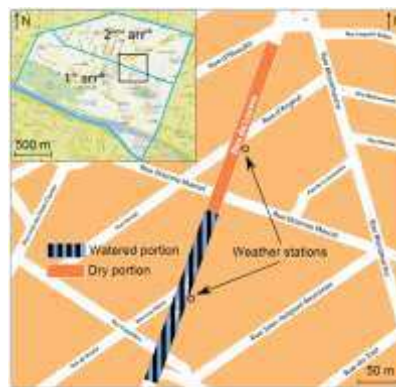
44 therefore important for decision-makers who face growing public pressure to reduce urban  
45 water use.

46 Several watering methods have been proposed or studied in the existing literature. In 2008,  
47 the City of Paris financed a numerical research program aimed at testing different climate  
48 change adaptation strategies for heat wave events [8]. This work analyzed a daytime  
49 pavement-watering method based on a hypothetical infrastructure connected to the city's non-  
50 potable water network. Pavements and sidewalks were watered at a rate of 0,2 *mm/h* for a  
51 duration of 3 minutes and frequency of every hour. During this work, a nighttime watering  
52 experiment was conducted over the summer of 2012 [9]. A single watering cycle of the  
53 pavement and sidewalk was conducted by cleaning truck around 10 pm sprinkling 1 *l/m<sup>2</sup>*,  
54 which is estimated by city officials as the maximum retention capacity of standard Parisian  
55 pavements. Field studies conducted in Nagoaka City, Japan used an existing snow-melting  
56 infrastructure which consists of a ground-water network used to water the road surface.  
57 Kinouchi & Kanda [1] ran this system continuously at a rate of 11 *mm/h*, while Takahashi et  
58 al. [3] ran it intermittently to deliver an average 2 *mm/h* with 3-minute sprinkles, every 30  
59 minutes. Yamagata et al. [4] used reclaimed waste water sprinkled onto a water-retentive  
60 pavement by temporary pipes placed on a central road planter. The watering method  
61 parameters are not specified in this study or in any of the other cited studies.

62 Of these, only Takahashi et al. [3] and Météo-France & CSTB [8] describe attempts to  
63 optimize the watering method with atmospheric cooling parameters. Takahashi et al. [3]  
64 optimize both watering rate and frequency based on surface and 90-cm air temperature  
65 observations over a period of one hour after watering. Météo-France & CSTB [8] base their  
66 own optimization on findings from Takahashi et al. with the hypothesis of a pavement water-  
67 holding capacity of 1 *mm*. They optimize the watering rate based on 2-m air temperature  
68 simulations with a one-hour time step.

69 We propose to optimize an adapted version of Bouvier et al.'s [9] pavement-watering  
70 method by studying the pavement's thermal behavior. We will demonstrate how pavement  
71 heat flux measurements can be used to fine-tune the watering frequency, and how a surface  
72 heat transfer analysis combined with a linear relation found between heat flux and solar  
73 irradiance during pavement insolation can provide information on the watering rate.  
74 Measurements were obtained from one of two experimental sites in Paris over the summer of  
75 2013. For this campaign, the rue du Louvre was equipped with a ground heat flux and  
76 temperature sensor which was placed 5 cm below the pavement surface as well as a  
77 pyranometer, and was watered several times during the day.

## 78 2. Materials and Methods



79  
80

Figure 1: Map of the rue du Louvre site

81 Conductive heat flux and surface temperatures were investigated on rue du Louvre, near  
 82 Les Halles in the 1<sup>st</sup> and 2<sup>nd</sup> Arrondissements in Paris, France over the summer of 2013.  
 83 Watered and control weather station positions are illustrated in Figure 1. Both watered and  
 84 dry portions of the street are approximately 180 m long and 20 m wide. Rue du Louvre has an  
 85 aspect ratio approximately equal to 1 and has a N-NE – S-SW orientation.

86 All data is presented in local daylight savings time (UTC +2). Statistical analyses were  
 87 conducted using the R software environment, version 3.0.1. Because the control site was  
 88 vandalized and thus rendered unoperational early during the experimental period, only  
 89 watered station data on watered and dry (control) days will be discussed hereafter.

90 **2.1. Instruments**

91 The pavement at each site was equipped with a thermo-fluxmeter at a depth of 5 cm. This  
 92 sensor was connected to a weather station which functioned continuously for the duration of  
 93 the summer and was used for additional microclimatic measurements which will not be  
 94 discussed here. Figure 2 illustrates a top view of sensor installation. The weather station was  
 95 positioned at the Eastern end of the cable.

96 The sensor was placed in the middle of the North-bound bus lane, causing no traffic  
 97 disturbances once installed. Unauthorized parking and a 100-m distant traffic light ensured  
 98 that only very limited shading or localized heat exhaust was caused by vehicles. Figure 3  
 99 shows a detailed cross-section of how the pavement sensor was set in place before filling.

100

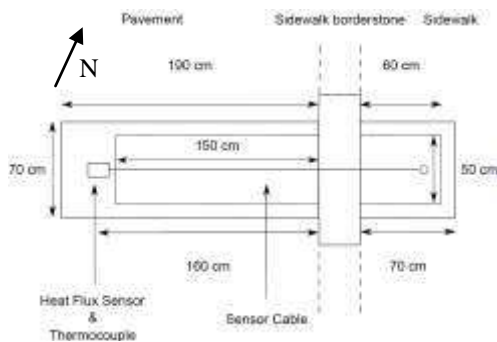


Figure 2: Top view of pavement sensor

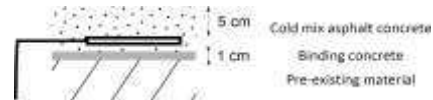


Figure 3: Cross-section detail of pavement sensor filling materials

101  
 102

Table 1 summarizes the instruments and data used for our upcoming analyses.

Parameter	Instrument	Height	Accuracy
Solar irradiance	Second Class Pyranometer ISO 9060	4 m	10% daily
Pavement heat flux	Taylor-made flowmeter	-5 cm	5%

103

Table 1: Instrument type, measurement height and accuracy

104 **2.2. Watering method and optimization goals**

105 Watering was started if certain weather conditions were met based on Météo-France's  
 106 three-day forecast. These as well as those for heat-wave warnings are presented in Table 2.

107 Cleaning trucks were used to sprinkle approximately 1 mm every hour from 6:30 am to  
 108 11:30 am and every 30 minutes from 2 pm until 6:30 pm on the sidewalk and pavement. This

109 is considered to be the maximum water-holding capacity of the pavement. Watering times  
 110 were reported by truck operators and cross-checked against visible images taken by a rooftop  
 111 thermal camera. Resulting watering time precision is estimated to be no better than 5 minutes.

112 Water used for this experiment was supplied by the city's 1,600-km non-potable water  
 113 network, principally sourced from the Ourcq Canal. Although water temperature was not  
 114 measured, its summertime range is reported by city services to be 20°-25°C.

115

Parameter	Pavement-watering	Heat-wave warning level
Mean 3-day minimum air temperature ( $BMI_{Min}$ )	> 16°C	> 21°C
Mean 3-day maximum air temperature ( $BMI_{Max}$ )	> 25°C	> 31°C
Wind speed	< 10 km/h	-
Sky conditions	Sunny (less than 2 oktas cloud cover)	-

116

Table 2: *Weather conditions required for pavement-watering and heat wave warnings*

117

In this situation, the goals we set for our pavement-watering optimization were:

118

- Maximize the obtained pavement cooling effect

119

- Minimize water consumption

120

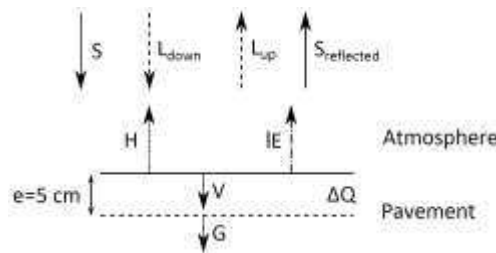
- Minimize the watering frequency to limit disturbances caused by cleaning trucks

121

Direct pavement heat flux analysis is sufficient for the frequency optimization, while a heat transfer analysis is necessary to estimate the effect of pavement-watering and to optimize the water consumption. The heat transfer analysis requires a preliminary analysis of pavement heat flux measurements.

124

### 125 2.3. Heat transfer analysis



126

127

Figure 4: *Diagram of pavement heat budget at surface*

128

For the rest of this article, we refer to pavement heat flux density at a depth of 5 cm as  $G$ , solar irradiance measured by the pyranometer at a height of 4 m as  $S'$  and that received by the pavement as  $S$ . All measurements are made at 1-minute intervals. Figure 4, based on Kinouchi & Kanda [2], shows a diagram of the heat fluxes relevant to this experiment. Heat absorption by the water film is not illustrated but is taken into account in the last item of equation (3).

130

131

132

Asaeda et al. [13] and Kinouchi & Kanda [2] characterize the energy balance of the pavement surface by the following equations:

133

$$R_n = S + L_{down} - L_{up} - S_{reflected} \quad (1)$$

134

$$R_n^{dry} = H^{dry} + V^{dry} \quad (dry) \quad (2)$$

137 
$$R_n^{wet} = H^{wet} + V^{wet} + lE + c\rho \frac{V_s}{t_0} (T_S^{wet} - T_W) \text{ (wet)} \quad (3)$$

138 
$$V = G + \Delta Q \quad (4)$$

139  $R_n$  is the net downward radiation received by the pavement surface and is the sum of the  
 140 downward solar irradiance  $S$ , downward longwave radiation  $L_{down}$  and upward longwave  
 141 radiation  $L_{up}$  and reflected shortwave radiation  $S_{reflected}$ ;  $H$  is the upward sensible heat flux;  $V$   
 142 is the downward pavement heat flux at the surface;  $l$  is the latent heat of vaporization for  
 143 water (2,260 J/g);  $E$  is the evaporation rate;  $c$  is the specific heat of water (4.18 kJ/kg.K);  $\rho$  is  
 144 the density of water (1,000 kg/m<sup>3</sup>);  $V_s$  is the water volume dispersed per unit surface area  
 145 (1 l/m<sup>2</sup>);  $t_0$  is the water cycle period in seconds;  $T_W$  is the water temperature;  $\Delta Q$  is the heat  
 146 storage flux by the first 5-cm layer of pavement.

147 According to Jurges' formula [14], convective heat flux can be written as:

148 
$$H = h(T_S - T_{air}) \quad (5)$$

149 Where  $T_S$  is the surface temperature of the pavement and  $T_{air}$  is that of the air above it.  $h$  is  
 150 the convective heat transfer coefficient.

151 Several empirical formulae exist to calculate  $h$  based on wind speed,  $v$  (in m/s). These  
 152 include  $h=6.15+4.18v$  used by Kusaka et al. [15] and  $h=5.7+3.8v$  in Duffie & Beckman [16].  
 153 Under our conditions,  $h$  is approximately equal to 10 W/m.K.

154 From these equations, the following can be derived when comparing dry and wet surface  
 155 conditions under equal insolation:

156 
$$lE + c\rho \frac{V_s}{t_0} (T_S^{wet} - T_W) = h(T_S^{dry} - T_S^{wet} + T_{air}^{wet} - T_{air}^{dry}) + V_{dry} - V_{wet} + L_{up}^{dry} - L_{up}^{wet} \quad (6)$$

157 From Stefan-Boltzmann law, we can express  $L_{up}$  as:

158 
$$L_{up} = \varepsilon\sigma T_S^4 \quad (7)$$

159  $\varepsilon$  is the emissivity of the emitting surface, while  $\sigma$  is Boltzmann's constant.

160 Therefore, knowledge of  $G$ ,  $\Delta Q$ , air, water and pavement surface temperatures under dry  
 161 and wet conditions allows an estimation of the latent heat flux and thus the evaporation rate.

## 162 2.4. Derivation of pavement solar irradiance from 4-meter solar irradiance

163  $S'$  was measured continuously starting on July 2<sup>nd</sup>, 2013. Because of the difference in  
 164 positioning of the pyranometer and the pavement sensor,  $S'$  is not equal to  $S$  and can therefore  
 165 not be used in its place for the heat transfer analysis. We must therefore derive  $S$  from  $S'$ .

166 Apart from possible insolation interruptions due to road traffic not visible in  $S'$ , the only  
 167 difference is the insolation period. The visible images taken by an infrared rooftop camera  
 168 reveal a 20-minute-long time lag between the beginning of pavement sensor and pyranometer  
 169 insolation during the month of July. The time lag is immediately identifiable when comparing  
 170 the graphs of  $G$  and  $S'$  for July 11<sup>th</sup> in Figure 5 and Figure 6. The beginning and end of  
 171 pavement and pyranometer insolation are illustrated by the two dotted and dashed vertical  
 172 lines in Figure 6, respectively. These coincide with the sudden increases and declines seen in  
 173 each signal. The insolation period of the pavement is approximately 1:35 pm to 6:30 pm,  
 174 while that of the pyranometer is 1:55 pm to 6:50 pm. We suppose that no signal distortion  
 175 other than the time lag is at play.

176 With these hypotheses, a modification of  $S'$  during the two 20-minute exclusive  
 177 disjunctions of pyranometer and pavement insolation is undertaken to obtain  $S$ . The rest of the

178 signal is unchanged, apart for distortions due to vehicles. Finally, to ensure signal continuity,  
 179 the 5 minutes following and/or preceding these 20-minute periods are also modified.

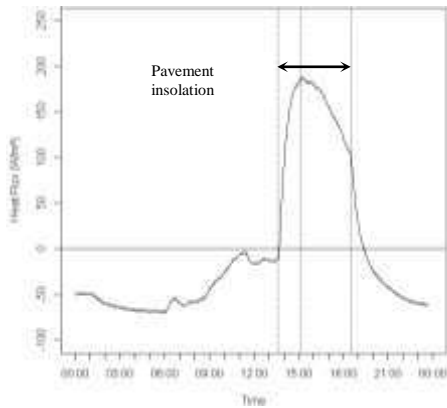


Figure 5:  $G$  measured on July 11<sup>th</sup>

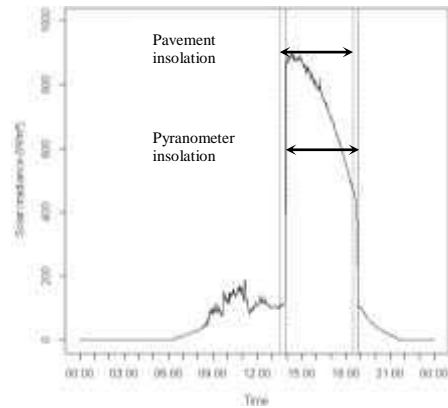


Figure 6:  $S'$  measured on July 11<sup>th</sup>

### 180 3. Watering period and frequency

181 Pavement heat flux density data from the watered station will now be compared between  
 182 watered days and days without watering (control days). These observations will help infer  
 183 conclusions on the watering frequency. All selected days are of Pasquill Stability Class A (i.e.  
 184 strong daytime insolation and surface wind speeds below 2 m/s) [17].

#### 185 3.1. Results

##### 186 3.1.1. Control days

187 The evolution of  $G$  and  $S$  on July 11<sup>th</sup>, 14<sup>th</sup>, and 20<sup>th</sup> are presented in Figure 7 through  
 188 Figure 12.  $S$  ranges from 0  $W/m^2$  to 120  $W/m^2$  during shading and from 120  $W/m^2$  to 900  $W/m^2$   
 189 during direct insolation.  $G$  ranges from -60  $W/m^2$  to 200  $W/m^2$ .

190 In terms of heat flux, each day can be divided into three periods: two of net heat release  
 191 ( $G < 0$ ) in the morning and evening and one of net heat storage ( $G > 0$ ) during the day. The net  
 192 release of heat by the pavement lasts about 18 hours, while heat is during the remaining 6  
 193 hours, approximately between 1:30 pm and 7 pm.

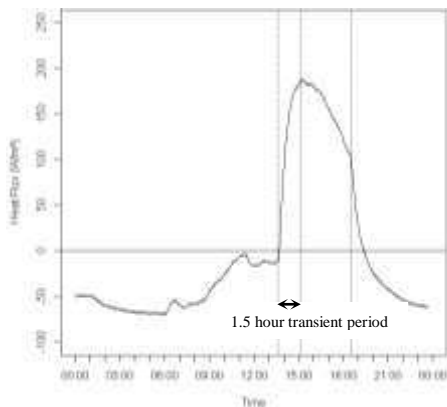


Figure 7:  $G$  measured on July 11<sup>th</sup>

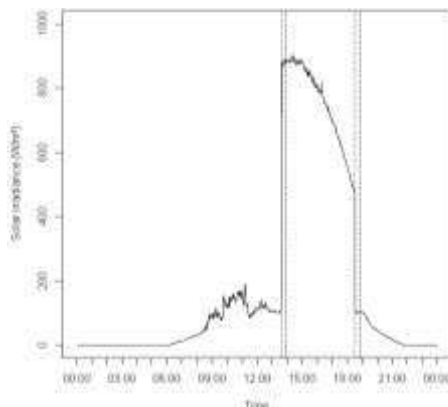


Figure 8:  $S$  measured on July 11<sup>th</sup>



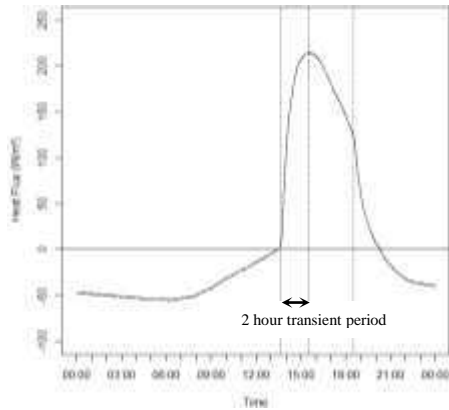


Figure 9:  $G$  measured on July 14<sup>th</sup>

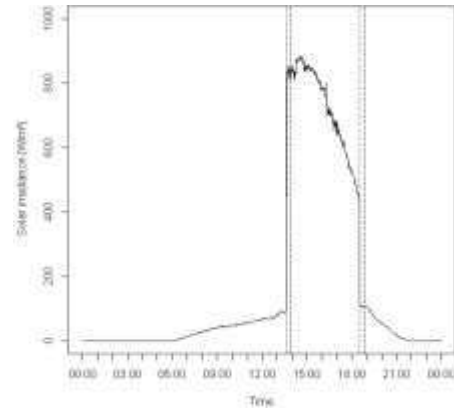


Figure 10:  $S$  measured on July 14<sup>th</sup>

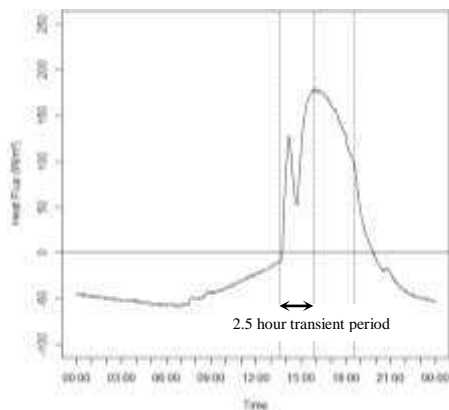


Figure 11:  $G$  measured on July 20<sup>th</sup>

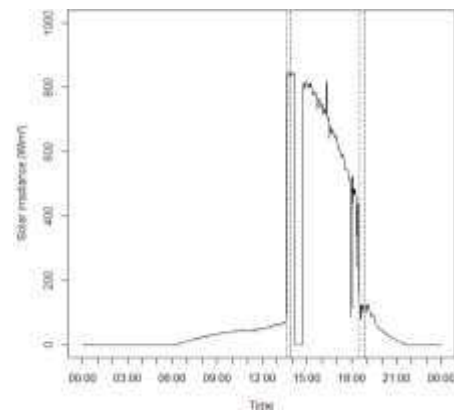


Figure 12:  $S$  measured on July 20<sup>th</sup>

195 When the sun starts to hit the pavement,  $G$  enters a transient period during which the top  
 196 5 cm layer of pavement begins to store heat, i.e. during which  $\Delta Q \neq 0$ . The transient period is  
 197 outlined by the first two dotted vertical lines in Figures 12, 14 and 16. The last dotted vertical  
 198 line indicates the instant when the pavement is shaded, at approximately 6:30 pm. After the  
 199 transient period,  $G$  and  $S$  follow a similar trend.

### 200 3.1.2. Watered days – July 8<sup>th</sup>, 10<sup>th</sup> and 22<sup>nd</sup>

201 Watered days will now be considered in the following order: July 8<sup>th</sup>, 22<sup>nd</sup> and 10<sup>th</sup>. Figure  
 202 13 through Figure 18 illustrate  $G$  and  $S$  on those dates, respectively. Dot-dashed vertical lines  
 203 represent watering cycles.  $S$  is in the same range as found on control days, while  $G$  ranges  
 204 from  $-75 \text{ W/m}^2$  to  $130 \text{ W/m}^2$ .

205 The maximum value of  $G$  is about half that reached on control days, ranging from  $70 \text{ W/m}^2$   
 206 to  $130 \text{ W/m}^2$ , approximately half that observed on control days. The daily peak in  $G$  is found  
 207 to coincide with the beginning of afternoon watering, except on July 10<sup>th</sup> when afternoon  
 208 watering began simultaneously to insolation. Furthermore, the observed reduction is inversely  
 209 proportional to the delay between the start of afternoon watering and the start of pavement  
 210 insolation. In other words, the later afternoon pavement-watering begins, the higher the daily  
 211 peak in  $G$ .

212 The watering methods applied in the afternoon on those dates and the daily maximum  
 213 value of  $G$  is summarized in Table 3. Watering cycles occurred at the specified frequencies  
 214 except for a 50-minute interruption on July 22<sup>nd</sup> at approximately 3 pm.

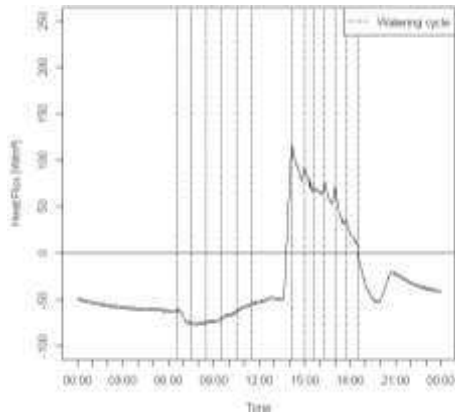


Figure 13: G measured on July 8<sup>th</sup>

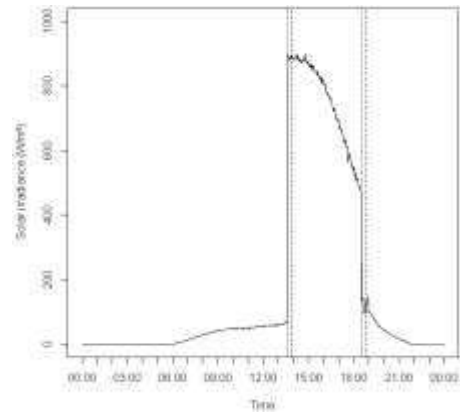


Figure 14: S measured on July 8<sup>th</sup>

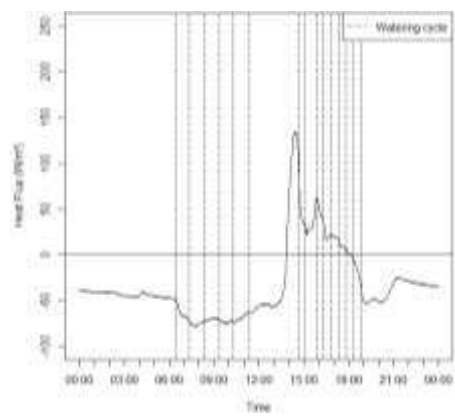


Figure 15: G measured on July 22<sup>nd</sup>

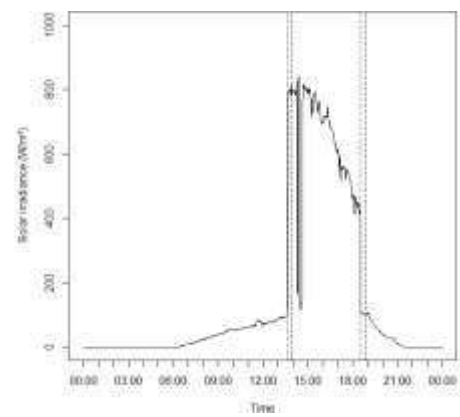


Figure 16: S measured on July 22<sup>nd</sup>

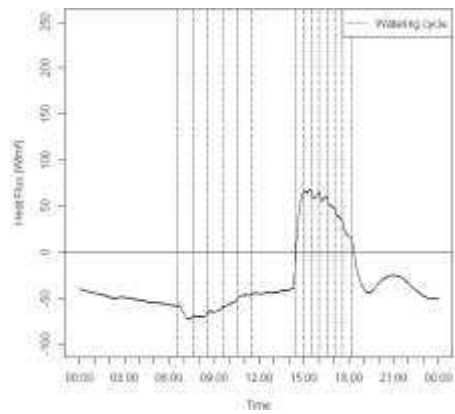


Figure 17: G measured on July 10<sup>th</sup>

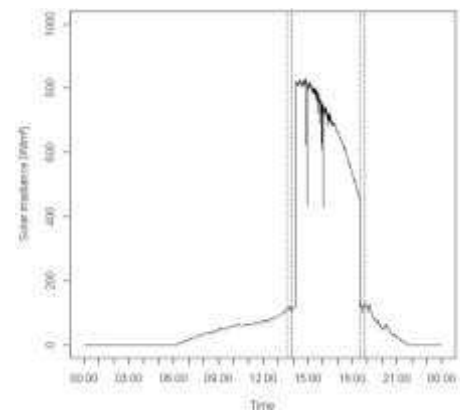


Figure 18: S measured on July 10<sup>th</sup>

215

Watering method parameter	July 8 <sup>th</sup>	July 22 <sup>nd</sup>	July 10 <sup>th</sup>
Watering rate (mm/h)	1.33	2	2
Watering period (minutes)	45	30	30
Delay of watering vs. start of insolation (minutes)	35	65	<5
Daily maximum value of G (W/m <sup>2</sup> )	115	130	70

216

Table 3: Actual watering method on considered watered days



217 Between 3 pm and 6:30 pm, the average reduction in pavement heat flux compared to  
 218 different reference control days is found to be between 100 and 150  $W/m^2$ . Table 4  
 219 summarizes these reductions. In the morning,  $G$  is reduced by approximately 15  $W/m^2$ .

220

Date	July 8 <sup>th</sup>		July 22 <sup>nd</sup>		July 10 <sup>th</sup>	
Control day (reference)	July 11 <sup>th</sup>	July 14 <sup>th</sup>	July 14 <sup>th</sup>	July 20 <sup>th</sup>	July 11 <sup>th</sup>	July 14 <sup>th</sup>
Average reduction ( $W/m^2$ )	-100	-120	-130	-150	-110	-130

221

Table 4: Average heat flux density reduction in  $W/m^2$  on watered days

222

223

224

225

226

227

222 Additionally, small heat flux spikes are observed in the afternoon on July 8<sup>th</sup> and 22<sup>nd</sup>.  
 223 Those that occur after the beginning of afternoon pavement-watering coincide with watering  
 224 cycles occurring 45 minutes or longer after the previous cycle. On July 10<sup>th</sup>, when watering is  
 225 conducted every 30 minutes without interruption, these spikes are significantly smaller than  
 226 on July 8<sup>th</sup> and 22<sup>nd</sup>. In the morning, no significant heat flux spikes are visible on watered  
 227 days, except for minor ones on July 10<sup>th</sup>.

228

229

230

231

232

228 Compared to control days, pavement-watering shortens the net heat storage period ( $G > 0$ )  
 229 by between 1 and 1.5 hours. This is caused by an earlier end of the net storage period, while  
 230 the beginning of heat storage is unaffected. On July 10<sup>th</sup>, pavement insolation was delayed by  
 231 a parked vehicle. Furthermore, pavement heat flux dips sharply at 6:30 pm when shading  
 232 begins and increases again 1-2 hours later, when the pavement surface dries.

233

### 3.2. Discussion

234

235

236

237

238

239

240

241

234 The comparison of  $G$  on watered days with control days revealed strong effects due to  
 235 pavement-watering. On the one hand, heat flux density reductions were found to be highest in  
 236 the afternoon during pavement insolation with  $G$  being more than halved. The average  
 237 reduction is between 100 and 150  $W/m^2$  during this period. Morning heat flux density, when  
 238 the pavement is shaded, was also reduced by pavement-watering in the order of 15  $W/m^2$ . On  
 239 the other hand, the daily peak in  $G$  was found to coincide with the first afternoon watering  
 240 cycle and to be proportional to the delay between this cycle and pavement insolation.  
 241 Furthermore, spikes in  $G$  were observed if watering cycles were more than 45 minutes apart.

242

243

244

245

246

242 This provides insight on two aspects of the watering method: its watering period and its  
 243 frequency. First, the value of the daily maximum of  $G$  depends on the start of afternoon  
 244 watering relatively to pavement insolation. Second, if the pavement watering frequency is too  
 245 low, the pavement surface has enough time to dry and  $G$  rises towards its normal control  
 246 value until the next watering cycle.

247

248

249

250

251

247 In order to maximize pavement cooling in the afternoon, watering should begin just a few  
 248 minutes prior to pavement insolation. Furthermore, the watering frequency must be adjusted  
 249 to prevent the pavement surface from drying. Our observations suggest that a period of 45  
 250 minutes is too long, while 30 minutes is nearly optimal during insolation. In the morning, in  
 251 shaded conditions, our data suggests that watering every hour is sufficient, perhaps optimal.

252

253

254

255

256

257

258

252 Overall, our observations are consistent with previous work. On control days, the trend in  
 253 heat flux is comparable to measurements made without pavement-watering by Kinouchi &  
 254 Kanda [2], also 5 cm deep, although inside a porous pavement. Our measurements are about  
 255 twice as large as what Asaeda et al. [13] observed 20 cm below the asphalt pavement surface.  
 256 Given the difference in depth, this discrepancy is not considered surprising. On watered days,  
 257 our observations are similar to those of Kinouchi & Kanda [1], [2] as well: the first watering  
 258 cycle on all watered days coincides with a small “nose-dive” in  $G$  in the order of 15  $W/m^2$ .

259 Lastly, the net storage period is shorter in our experiment than in reports from Kinouchi &  
 260 Kanda [2] or Asaeda et al. [13], but they were working in nearly unmasked conditions.

261 **4. Watering rate**

262 Kinouchi & Kanda [2] put into perspective a correlation between  $R_n$  and  $G$ . They  
 263 proceeded by plotting  $G$  as a function of  $R_n$ . Camuffo & Bernardi [18] explore the hysteresis  
 264 cycles found between surface heat fluxes and net radiation for soil. Other authors such as  
 265 Asaeda et al. [13], studying the effect of pavement heat storage on the lower atmosphere, also  
 266 look into this hysteresis cycle for asphalt and concrete pavements. Because we did not measure  
 267 net radiation, we shall proceed in an analogous fashion with  $S$  instead. This will allow us to  
 268 estimate the surface cooling effect of pavement watering based on a relation between  $S$  and  $G$   
 269 during pavement insolation. From this we get an estimate of the evaporation rate and  
 270 therefrom we can make recommendations on the watering rate.

271 **4.1. Results**

272 Figure 19 through Figure 24 show  $G$  as a function of  $S$  on July 11<sup>th</sup>, 14<sup>th</sup>, 20<sup>th</sup>, 8<sup>th</sup>, 22<sup>nd</sup> and  
 273 10<sup>th</sup>, respectively. The chronological order of the data points is anti-clockwise. The least  
 274 square regression line of  $G$  according to  $S$  between 3 pm and 6:30 pm is plotted for each date.

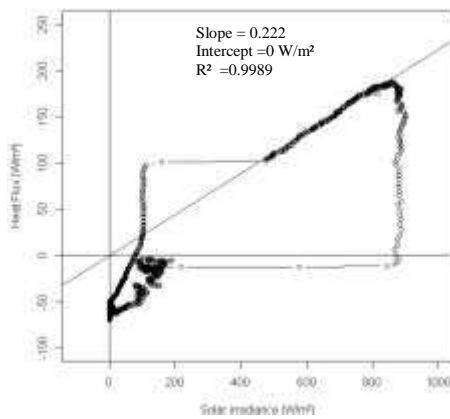


Figure 19:  $G$  as a function of  $S$  on July 11<sup>th</sup>

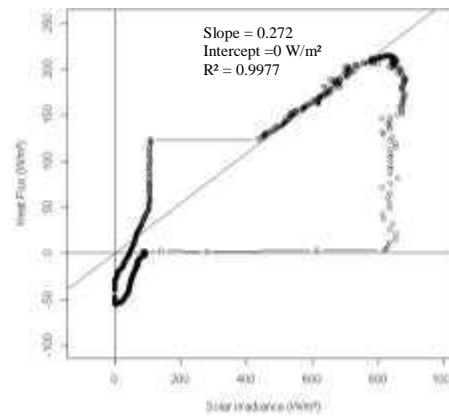


Figure 20:  $G$  as a function of  $S$  on July 14<sup>th</sup>

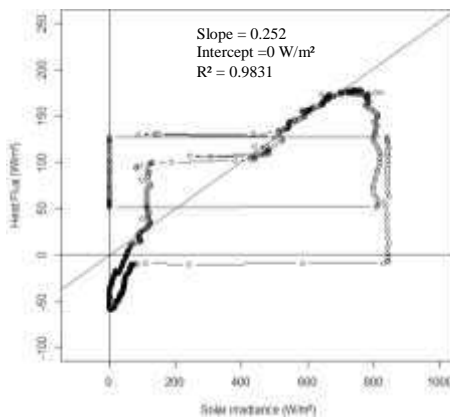


Figure 21:  $G$  as a function of  $S$  on July 20<sup>th</sup>

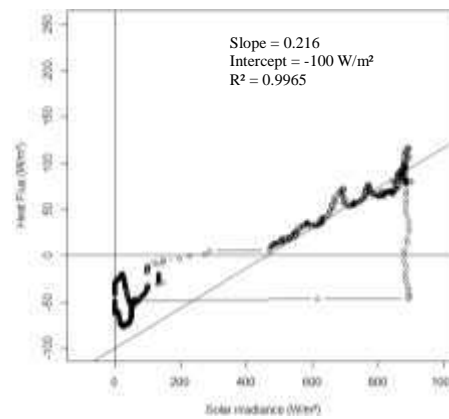


Figure 22:  $G$  as a function of  $S$  on July 8<sup>th</sup>

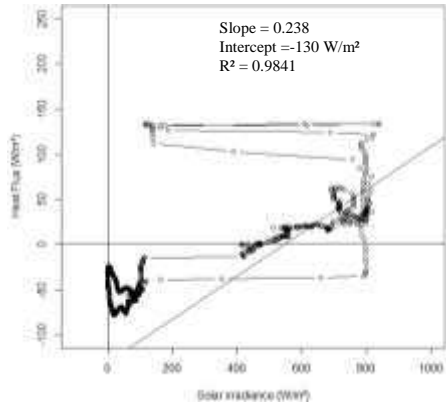


Figure 23:  $G$  as a function of  $S$  on July 22<sup>nd</sup>

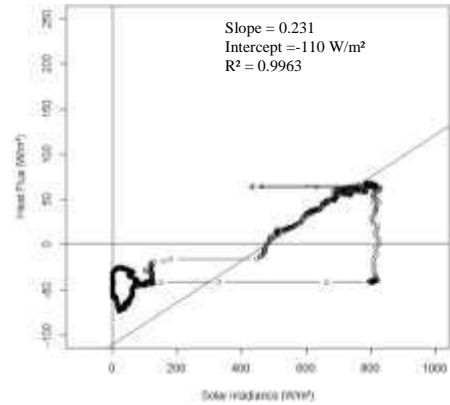


Figure 24:  $G$  as a function of  $S$  on July 10<sup>th</sup>

276 The parameters from the linear regression can be formalized as:

277 
$$G = \alpha S + G_0 \tag{8}$$

278  $\alpha$  is the conversion coefficient of solar irradiance to pavement heat flux 5 cm below the  
 279 pavement surface, while  $G_0$  is the intercept heat flux under these conditions.

280 The regressions were conducted for control and watered days. On control days, an  
 281 intercept of  $0 \text{ W/m}^2$  was used. Table 5 summarizes the regression parameters for control days.

282

Date	July 11 <sup>th</sup>	July 14 <sup>th</sup>	July 20 <sup>th</sup>
$\alpha$	0.222	0.272	0.252
$R^2$	0.9989	0.9977	0.9831

283

Table 5:  $\alpha$  and  $R^2$  on control days

284 Each fit is statistically significant, with coefficients of determination in excess of 0.98.  
 285 Overall, the conversion coefficients derived on control days range from 22% to 27%.

286 On watered days, different intercepts, corresponding to the average reduction of  $G$  found in  
 287 Table 4, were tested. Using these intercepts, similar slopes to those found on control days  
 288 were obtained. Table 6 summarizes the regression parameters using the different intercepts for  
 289 watered days.

290 Regardless of the intercept value used, the conversion coefficients deviate only slightly  
 291 from those derived on control days, remaining in the same 22-27% range.

292

Date	July 8 <sup>th</sup>		July 22 <sup>nd</sup>		July 10 <sup>th</sup>	
	July 11 <sup>th</sup>	July 14 <sup>th</sup>	July 14 <sup>th</sup>	July 20 <sup>th</sup>	July 11 <sup>th</sup>	July 14 <sup>th</sup>
$G_0$ ( $\text{W/m}^2$ , user-input)	-100	-120	-130	-150	-110	-130
$\alpha$	0.216	0.244	0.238	0.269	0.231	0.261
$R^2$	0.9965	0.9955	0.9861	0.9849	0.9959	0.9953

293

Table 6:  $\alpha$ ,  $R^2$  and  $G_0$  on watered days

294 Considering the statistical significance of these regression parameters, we conclude that  
 295 pavement-watering does not significantly affect the conversion coefficient, i.e. how solar  
 296 energy is transmitted 5 cm deep into the pavement, but adds a constant negative heat flux,  $G_0$ .

297 Based on observations by Kinouchi & Kanda [2] and this unmodified conversion rate, we  
 298 shall assume that  $\Delta Q$  is also unchanged by watering during insolation, i.e.  $\Delta Q^{wet} = \Delta Q^{dry}$ .

299 This information allows us to estimate the cooling created by the sprinkled water. We find  
 300 that the contribution from water advection is between 23 and 35  $W/m^2$ , while that of  
 301 evaporation is 304-375  $W/m^2$ . This is produced by the evaporation of 0.48 to 0.60  $mm/h$ .  
 302 Advection is therefore responsible for less than 10% of observed cooling while it is provided  
 303 by up to three times more water than evaporative cooling.

304 This is derived by using the regression parameters to express  $G$  as a linear function of  $S$   
 305 during steady state insolation conditions:

$$306 \quad G = \alpha S + G_0 \delta_{wet} \quad (9)$$

307 In equation (9),  $\delta_{wet}$  is the wet pavement indicator function. In dry surface conditions,  
 308  $\delta_{wet} = 0$ , while in wet surface conditions  $\delta_{wet} = 1$ .

309 Integrating equations (7) and (9) into (6), we obtain:

$$310 \quad lE + c\rho \frac{V_s}{t_0} (T_S^{wet} - T_W) = h(T_S^{dry} - T_S^{wet} + T_{air}^{wet} - T_{air}^{dry}) - G_0 + \sigma (\varepsilon_d T_S^{dry^4} - \varepsilon_w T_S^{wet^4}) \quad (10)$$

311 As stated in the introduction, previous studies of pavement-watering report air temperature  
 312 reductions of up to 4°C [1]–[4], [9]. For our analysis, we assume that  $-2^\circ C \leq T_{air}^{wet} - T_{air}^{dry} \leq 0$

313 In addition, collected pavement surface temperature data (not discussed here) reveal an  
 314 average reduction during insolation of 15°C, from 323 K to 308 K. Having assumed that  
 315  $h = 10 W/m^2.K$ , and considering that  $110 W/m^2 \leq -G_0 \leq 150 W/m^2$  on days with the  
 316 optimal 30-minute watering, we obtain:

$$317 \quad 339 W/m^2 \leq lE + c\rho \frac{V_s}{t_0} (T_S^{wet} - T_W) \leq 399 W/m^2$$

318 As stated previously, we know from past non-potable water analyses conducted by the city  
 319 services that its temperature is usually in the 20-25°C range on hot summer days. Assuming  
 320 that the runoff temperature increases to 35°C by contact with the pavement, we obtain:

$$321 \quad \begin{cases} 23 W/m^2 \leq c\rho \frac{V_s}{t_0} (T_S^{wet} - T_W) \leq 35 W/m^2 \\ 304 W/m^2 \leq lE \leq 375 W/m^2 \end{cases}$$

322 Considering a latent heat of evaporation of 2,260  $kJ/kg$ , we can assert that the evaporation  
 323 rate is between 0.134 and 0.166  $g/m^2.s$ , i.e. between 0.48 and 0.60  $mm/h$ . This means that for  
 324 each 30-minute watering cycle, 0.24 to 0.30  $mm$  evaporate. Since we know from our  
 325 preliminary pavement heat flux analysis that the pavement dries off after 30 minutes, we can  
 326 assert that the rest of the water runs off into the sewer system.

## 327 4.2. Discussion

328 The analysis of  $G$  as a function of  $S$  during insolation after the initial transient period has  
 329 allowed us to demonstrate that pavement-watering accounts for 339 to 399  $W/m^2$  of pavement  
 330 surface cooling. At least 90% of total cooling attributable to pavement-watering is produced  
 331 by evaporation, up to 10% being produced by water advection.

332 The relative contributions of advection and evaporation contrast strongly with the amount  
333 of water used by each of these phenomena which is respectively 2 *mm/h* and 0.48 to  
334 0.60 *mm/h*. Pavement cooling by water advection is therefore much less water efficient than  
335 that from evaporation: 12 to 18  $W/m^2$  of cooling per 1 *mm/h* of sprinkled water, compared to  
336 628  $W/m^2$  per 1 *mm/h* of evaporated water.

337 Since evaporative cooling cannot be increased by adding more water, increasing the  
338 watering rate further would only increase the advective contribution. However, in light of its  
339 low cooling efficiency, this is unadvisable for our optimization goal. On the contrary, we  
340 would recommend lowering the watering rate to match the evaporation rate exactly. This  
341 would lower advective cooling to between 6 and 10  $W/m^2$ , bringing total pavement-watering  
342 cooling down to between 309 and 386  $W/m^2$ , i.e. a 3-9% reduction for a 70-76% water saving.

343 Our estimations of latent heat flux are consistent with those reported by Météo-France &  
344 CSTB [8] who find that latent heat flux can reach 300  $W/m^2$ . Furthermore, they found an  
345 optimal watering rate of 0.2 *mm/h* for all of Paris' road surfaces. This value was obtained by  
346 testing different watering rates with a frequency of every hour and a water-holding capacity of  
347 1 *mm*. However, it is a daily and city average for watering every hour between 5 am and 7 pm  
348 and is not more accurately defined for individual street configurations. Furthermore, the  
349 authors were limited in the choice of the watering frequency since the model's time step was  
350 one hour and was found sufficient considering a water-holding capacity of 1 *mm*. Our  
351 findings are therefore consistent with theirs.

352 Another consequence of our results is information on the water-holding capacity of the  
353 pavement. Since the pavement dries 30 minutes after watering during insolation, the water-  
354 holding capacity of the pavement is therefore equal to the amount of water evaporated in  
355 between 30-minute watering cycles, i.e. between 0.24 and 0.30 *mm*. This is significantly less  
356 than that assumed by Météo-France & CSTB [8], but is only valid for the portion of pavement  
357 surveyed by the heat flux sensor. This portion has a specific geometric configuration and  
358 surface composition (cold- versus hot-mix asphalt concrete). However, we can still assert that  
359 the optimized watering method applies the exact water-holding capacity of the target  
360 pavement-area at the frequency that it takes for that amount of water to completely evaporate.  
361 Thus, if we assume that the watering frequency used in the morning is optimal, we can  
362 estimate morning evaporation to 0.24 to 0.30 *mm/h*.

363 Sources of uncertainty in our estimations lie in the use of  $S$  rather than  $R_n$ , the  
364 approximation of the convective heat transfer coefficient  $h$  and our assumptions regarding  
365 water temperature, air temperature changes and the storage heat flux density in dry and wet  
366 conditions. Concerning the latter, observations over several days by Kinouchi & Kanda [2]  
367 suggest that  $\Delta Q$  is unaffected by pavement watering under identical insolation conditions.

## 368 **5. Conclusion**

369 The field study conducted on rue du Louvre in Paris over the summer of 2013 has allowed  
370 us to expose the thermal effects of pavement-watering on a pavement area located 1.6 m away  
371 from the eastern sidewalk in a street with an aspect ratio of  $H/W=1$  and of N-NE – S-SW  
372 orientation. Pavement heat flux density at 5 cm depth was found to be more than halved by  
373 pavement-watering during insolation, while a heat transfer analysis based on a linear relation  
374 found between solar irradiance and heat flux density allowed us to estimate evaporative  
375 cooling to between 304 and 375  $W/m^2$ , representing at least 90% of total pavement-watering  
376 cooling. This translates to an evaporation rate of between 0.48 and 0.60 *mm/h*. Assuming that  
377 the one-hour morning watering cycles were optimal, the evaporation rate during morning

378 shaded conditions is 0.24 to 0.30 mm/h. Finally, we found that the water-holding capacity of  
379 the surveyed pavement zone is 0.24 to 0.30 mm.

380 Based on these analyses, we recommend watering the exact water-holding capacity of the  
381 pavement at the lowest possible frequency that prevents the pavement from drying. In our  
382 case, this translates to 30-minute watering cycles with a watering rate of 0.48 to 0.60 mm/h  
383 during pavement insolation. In the morning, 60-minute watering cycles and a watering rate of  
384 0.24 to 0.30 mm/h are recommended. Compared to our experiment, this watering method  
385 would use 76% less water while still providing at least 90% of observed pavement cooling.  
386 Finally, the watering period should include a few minutes right before pavement insolation to  
387 maximize the cooling effect.

388 In order to reduce the watering frequency further and thus cause less disturbance  
389 associated with watering cycles, the pavement water-holding capacity would need to be  
390 increased. As Parisian streets are currently designed to evacuate surface water as fast as  
391 possible, a change in street design is necessary to meet this objective. One alternative that can  
392 be considered is to use water-retaining pavement materials. The new street material would  
393 have to store water at or near its surface without preventing evaporation. Such a material  
394 would permit the delivery of larger amounts of water per watering cycle with lower runoff  
395 and thus reduce the watering frequency. In addition, the new road structure may be able to  
396 store rainfall from summer storms or water already used for street cleaning long enough for  
397 evaporation on hot days. This would lead to additional water savings all while having positive  
398 impacts on rainwater runoff management.

399 Water temperature, net radiation and sensible heat flux measurements as well as the  
400 determination of the thermal characteristics of the pavement material would help address the  
401 sources of uncertainty in our analysis. In addition, these measurements would allow us to  
402 verify our conjecture on optimal watering during pavement shading via a similar approach to  
403 that used for the afternoon.

#### 404 **References**

- 405 [1] T. Kinouchi and M. Kanda, "An Observation on the Climatic Effect of Watering on Paved  
406 Roads," *J. Hydrosoci. Hydraul. Eng.*, vol. 15, no. 1, pp. 55–64, 1997.
- 407 [2] T. Kinouchi and M. Kanda, "Cooling Effect of Watering on Paved Road and Retention in  
408 Porous Pavement," in *2nd Symposium on Urban Environment*, 1998, pp. 255–258.
- 409 [3] R. Takahashi, A. Asakura, K. Koike, S. Himeno, and S. Fujita, "Using Snow Melting Pipes to  
410 Verify the Water Sprinkling's Effect over a Wide Area," in *NOVATECH 2010*, 2010, p. 10.
- 411 [4] H. Yamagata, M. Nasu, M. Yoshizawa, A. Miyamoto, and M. Minamiyama, "Heat island  
412 mitigation using water retentive pavement sprinkled with reclaimed wastewater.," *Water Sci.  
413 Technol.*, vol. 57, no. 5, pp. 763–71, Jan. 2008.
- 414 [5] T. Nakayama and T. Fujita, "Cooling effect of water-holding pavements made of new materials  
415 on water and heat budgets in urban areas," *Landsc. Urban Plan.*, vol. 96, no. 2, pp. 57–67, May  
416 2010.
- 417 [6] T. Nakayama, S. Hashimoto, and H. Hamano, "Multiscaled analysis of hydrothermal dynamics  
418 in Japanese megalopolis by using integrated approach," *Hydrol. Process.*, vol. 26, no. 16, pp.  
419 2431–2444, Jul. 2012.
- 420 [7] J. He and A. Hoyano, "A numerical simulation method for analyzing the thermal improvement  
421 effect of super-hydrophilic photocatalyst-coated building surfaces with water film on the  
422 urban/built environment," *Energy Build.*, vol. 40, no. 6, pp. 968–978, Jan. 2008.
- 423 [8] Météo-France and CSTB, "EPICEA - Rapport final," 2012.
- 424 [9] M. Bouvier, A. Brunner, and F. Aimé, "Nighttime watering streets and induced effects on the  
425 surrounding refreshment in case of hot weather. The city of Paris experimentations," *Tech. Sci.  
426 Méthodes*, no. 12, pp. 43–55 (In French), 2013.

- 427 [10] J. Nicolas, "Reducing the urban heat island effect," *Le Moniteur*, 2013. [Online]. Available:  
 428 [http://www.lemoniteur.fr/133-amenagement/article/actualite/22580961-experimentation-](http://www.lemoniteur.fr/133-amenagement/article/actualite/22580961-experimentation-reduire-l-effet-d-ilot-de-chaueur-urbain)  
 429 [reduire-l-effet-d-ilot-de-chaueur-urbain](http://www.lemoniteur.fr/133-amenagement/article/actualite/22580961-experimentation-reduire-l-effet-d-ilot-de-chaueur-urbain). [Accessed: 22-Jan-2014].
- 430 [11] A. Lemonsu, R. Kounkou-Arnaud, J. Desplat, J.-L. Salagnac, and V. Masson, "Evolution of the  
 431 Parisian urban climate under a global changing climate," *Clim. Change*, vol. 116, no. 3–4, pp.  
 432 679–692, Jul. 2012.
- 433 [12] J.-M. Robine, S. L. K. Cheung, S. Le Roy, H. Van Oyen, C. Griffiths, J.-P. Michel, and F. R.  
 434 Herrmann, "Death toll exceeded 70,000 in Europe during the summer of 2003.," *C. R. Biol.*,  
 435 vol. 331, no. 2, pp. 171–8, Feb. 2008.
- 436 [13] T. Asaeda, V. T. Ca, and A. Wake, "Heat storage of pavement and its effect on the lower  
 437 atmosphere," *Atmos. Environ.*, vol. 30, no. 3, pp. 413–427, Feb. 1996.
- 438 [14] W. Jürges, "Die Wärmeübergang an einer ebenen Wand," *Beihefte zum Gesundheits-Ingenieur*,  
 439 vol. 19, no. 1, pp. 1227–1249, 1924.
- 440 [15] H. Kusaka, H. Kondo, and Y. Kikegawa, "A simple single-layer urban canopy model for  
 441 atmospheric models : comparison with multi-layer and slab models," *Boundary-Layer*  
 442 *Meteorol.*, vol. 101, no. 3, pp. 329–358, 2001.
- 443 [16] J. A. Duffie and W. A. Beckman, *Solar Engineering of Thermal Processes*, 2nd Editio. New  
 444 York, 1991, p. 944.
- 445 [17] F. Pasquill, "The estimation of the dispersion of windborne material," *Meteorol. Mag.*, vol. 90,  
 446 no. 1063, pp. 33–49, 1961.
- 447 [18] D. Camuffo and A. Bernardi, "An observational study of heat fluxes and their relationships  
 448 with net radiation," *Boundary-Layer Meteorol.*, vol. 23, no. 3, pp. 359–368, Jul. 1982.

449

## 450 Acknowledgements

451 The authors would like to thank APUR for lending their Flir TiR32 infrared camera and  
 452 Orange for allowing the use of their rooftop terrace located at 46, rue du Louvre for  
 453 instruments used during this experiment. They also acknowledge the support of Météo-France  
 454 and APUR as well as the Green Spaces and Environment, Roads and Traffic and the Waste  
 455 and Water Divisions of the City of Paris during the preparation phase of this experiment.

456 Funding for this experiment was provided for by the Water and Sanitation Department of  
 457 the City of Paris.

## 458 Nomenclature

459	$\alpha$	conversion coefficient of solar irradiance to pavement heat flux density at 5 cm depth, -
460	APUR	Parisian urban planning agency
461	$BMI_{Min}$	Minimum biometeorological index, 3-day mean of daily low temperature, °C
462	$BMI_{Max}$	Maximum biometeorological index, 3-day mean of daily high temperature, °C
463	$c$	water specific heat, 4.18 J/g.K
464	$\Delta Q$	storage heat flux density by top 5-cm layer of pavement, W/m <sup>2</sup>
465	$e$	pavement thickness above the heat flux sensor, 5 cm
466	$E$	evaporation rate, g/s
467	$\varepsilon_d$	dry pavement emissivity, 0.97
468	$\varepsilon_w$	wet pavement emissivity, 0.98
469	$G$	downward conductive heat flux density, 5 cm below the pavement surface, W/m <sup>2</sup>
470	$H$	upward sensible heat flux density at pavement surface, W/m <sup>2</sup>
471	$h$	convection coefficient, W/m <sup>2</sup> .K
472	$\ell$	latent evaporation heat of water, 2,260 kJ/kg
473	$L_{down}$	downward longwave radiation density, W/m <sup>2</sup>
474	$L_{up}$	upward longwave radiation density, W/m <sup>2</sup>
475	MRT	mean radiant temperature, °C
476	$R_n$	net radiation density, W/m <sup>2</sup>
477	$\rho$	water density, 1,000 kg/m <sup>3</sup>
478	$S$	pavement solar irradiance, W/m <sup>2</sup>



479	$S'$	pyranometer solar irradiance, $W/m^2$
480	$S_{reflected}$	reflected shortwave radiation density, $W/m^2$
481	$T_{air}$	atmospheric air temperature, $^{\circ}C$
482	$T_S$	pavement surface temperature, $^{\circ}C$
483	$T_w$	water temperature, $^{\circ}C$
484	$t_0$	watering cycle period, <i>hours</i>
485	$V$	pavement conductive heat flux density, at surface, $W/m^2$
486	$UHI$	urban heat island